Texture features based on local Fourier histogram: self-compensation against rotation

Ahsan Ahmad Ursani,[a,b] Kidiyo Kpalma,[a] and Joseph Ronsin[a]
[a]IETR, Image and Remote Sensing Group, INSA de Rennes, 20, Avenue des Buttes de Coësmes, 35043 Rennes Cedex, France
[b]IICT, Mehran University of Engineering & Technology, Jamshoro 76062 Sindh, Pakistan
E-mail: aursani@ens.insa-rennes.fr

Abstract. *We present a method of introducing rotation invariance in texture features based on a local Fourier histogram (LFH) computed using a 1-D discrete Fourier transform (DFT). To compensate for image rotation, a local image-gradient angle at each image pixel is found from within one of the 1-D DFT coefficients. The rotation invariance is established theoretically, analytically as well as empirically. The rotation-compensated features extracted from the same texture image oriented at different angles exhibit very high cross correlation. Therefore, the proposed texture features are expected to yield very high accuracies for a variety of image data and applications. The improved LFH-based features outperform the earlier version of the features and the features based on Gabor filters in texture recognition on 8560 images from the Brodatz album. © 2008 SPIE and IS&T.* [DOI: 10.1117/1.2965439]

1 Introduction

Texture features play an important role in several image-processing applications ranging from computer vision and medical image processing to remote sensing and content-based image retrieval. Almost all the texture processing applications require rotation invariance in the texture features, which we achieve here in a very simple and cost-effective manner. Reference 1 categorizes the wide range of texture features proposed to date into two broad categories and compares them: features that use a large bank of filters or wavelets and features that use immediate pixel neighborhood properties. It shows that the latter outperforms the former. Hence, we take on improving a feature set from the latter category. In Ref. 2, texture features are extracted using a 1-D discrete Fourier transform (DFT) of the circular neighborhood around a pixel. It proposes computing a 1-D DFT of the 8-pixel sequence around each image pixel and uses magnitudes of the DFT coefficients to extract texture features. More recent work[3] extracts similar texture features from the square neighborhood and calls it a local Fourier histogram (LFH)-based feature set. The LFH-based feature set was shown to perform better than the texture features extracted from a large filter bank of Gabor filters,[4] which are computationally more expensive than the LFH-based features. In this work, we augment the LFH-based feature set by using the phases of the DFT coefficients as texture features as well. However, the improvement suggested herein equally applies to the texture features extracted from the circular neighborhood.[2] Since the phases are sensitive to image rotation, we also present a method to make them rotation invariant. This does not cause any additional computational cost, but does improve performance.

The following sections explain how the LFH-based features are extracted, how the local image gradient angle is determined from the features themselves, and how the image gradient angle is used to compensate the features against rotation. Results are presented before concluding the paper.

2 Method of Extracting DFT-Based Texture Features

The texture features proposed in Ref. 3 are extracted in the spatial domain by taking a 1-D DFT of the 8-pixel sequence x_0 through x_7, hereafter called x, around a central pixel as shown in Fig. 1. We use the local image gradient at the central pixel to compensate the extracted features for the effects of image rotation.

When moving a 3×3 pixel window across a texture image, the 1-D DFT of x is computed as

$$X_k = \sum_{n=0}^{7} x_n \exp\left(-\frac{\pi i}{4}kn\right), \tag{1}$$

where $0\le k\le 7$, X_k represents the k'th Fourier coefficient, and x_n represents the n'th value in x. From the computed DFT, histograms of the absolute values of the first five DFT coefficients, i.e., $|X_0|$ through $|X_4|$, were used for texture description in Ref. 3

The phases of the DFT coefficients X_1 through X_3 were also proposed as features in Ref. 3 but only for those applications that do not deal with image rotation. The phase features were otherwise excluded because, unlike magnitudes, the phases of the DFT coefficients are sensitive to image rotation. Reference 2 also proposes only magnitudes of the DFT coefficients as texture features. We propose using the histograms of phases of X_2 and X_3 after appropriately compensating with the local image gradient.

2.1 *Local Image Gradient*

Traditionally, as a good compromise between cost and accuracy, the 3×3-pixel edge-detection operators such as the Sobel (SO) and Prewitt operators (PO)are often used to estimate local image gradient at a given pixel. Below are

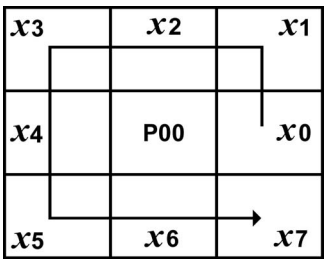

Fig. 1 9-pixel neighborhood in the spatial domain.

Paper 08013LRR received Jan. 25, 2008; revised manuscript received Jun. 19, 2008; accepted for publication Jun. 23, 2008; published online Aug. 5, 2008.

1017-9909/2008/17(3)/030503/3/$25.00 © 2008 SPIE and IS&T.

Table 1 XCC between the histograms of ϕ_2 and ϕ_3, respectively, corresponding to images oriented at 0 deg and to those at 30, 45, 60, and 90 deg averaged over all the images from the Brodatz album.

		Cross correlation coefficient			
	Orientation (deg)	30	45	60	90
Phase feature	ϕ_2	0.979	0.988	0.984	0.987
	ϕ_3	0.918	0.907	0.923	0.997

the general 3×3 edge-detection operators in which the value of b varies from 1, as in the PO, to 2, as in the SO:

$$S_X=\begin{bmatrix}-1 & 0 & 1\\ -b & 0 & b\\ -1 & 0 & 1\end{bmatrix},\quad S_Y=\begin{bmatrix}-1 & -b & -1\\ 0 & 0 & 0\\ 1 & b & 1\end{bmatrix}, \tag{2}$$

where S_X and S_Y are convolved with a texture image to obtain two gradient images, G_X and G_Y, respectively. The local image gradient angle δ is calculated as

$$\delta=\tan^{-1}\left(\frac{G_Y}{G_X}\right). \tag{3}$$

Convolving the edge detection operators of Eq. (2) with the 3×3-pixel neighborhood of Fig. 1 gives G_Y and G_X, which are substituted in Eq. (3) giving

$$\tan\delta=\frac{-x_1-bx_2-x_3+x_5+bx_6+x_7}{bx_0+x_1-x_3-bx_4-x_5+x_7}. \tag{4}$$

However, the local image-gradient angle can also be obtained from the phase of the first coefficient $\angle X_1$ of the DFT of x. By substituting $k=1$ in Eq. (1) gives

$$\tan\angle X_1=\frac{-x_1-\sqrt{2}x_2-x_3+x_5+\sqrt{2}x_6+x_7}{\sqrt{2}x_0+x_1-x_3-\sqrt{2}x_4-x_5+x_7}. \tag{5}$$

Equations (4) and (5) happen to be exactly the same if $b=\sqrt{2}$ and they are very similar otherwise, because the value $\sqrt{2}$ falls between the usual values of 1 and 2. For instance, the histograms of the local image-gradient angle from $\angle X_1$ and from the SO ($b=2$) for image D87 of the Brodatz album (BA) have a cross-correlation coefficient (XCC) of 0.97. In addition, if we consider the $\angle X_1$ image as a noisy version of the SO-driven image, the signal-to-noise ratio (SNR) is 69 dB, verifying that the former is a very close approximation of the latter. All other images of the album were tested, and more or less similar values of correlation coefficient and SNR were found between the two approximations of the image gradient. Hence, instead of computing the local image-gradient angle using any 2-D edge-detection operators, we use the value $\angle X_1$ to compensate the phases of the two other DFT coefficients, i.e., $\angle X_2$ and $\angle X_3$, against the effects of image rotation. It can now be said that $\delta=\angle X_1$.

2.2 *Effects of Image Rotation on Fourier Coefficients*

Consider that an image is rotated by an arbitrary angle, with the center of rotation exactly in the middle of the image. The angle of rotation at any other point P_{xy} on the image would be different from what it is at the center of rotation. Let the angle of rotation be ψ deg at point P_{00} (see Fig. 1), corresponding to a shift in the string x by m places. This shift in x causes nothing but the changes in the phases of the resulting DFT coefficients. Equation (6) states the shift property of DFT:

$$F[(x_{n-m})]_k=F[(x_n)]_k\exp\left(-\frac{\pi i}{4}km\right), \tag{6}$$

where $F[(x_n)]_k$ represents the k'th coefficient of the DFT of (x_n), and $F[(x_{n-m})]_k$ represents the k'th coefficient of the DFT of the string (x_{n-m}) that is the same string (x_n) shifted by m places. Equation (6) shows that any displacement in time or space domain causes a phase shift given by

Table 2 Recognition rates relative to Orientation with 8560 Brodatz images.

		% Accuracy						
	Orientation (deg)	0	30	45	60	90	Avg.	RV
Feature set	LFT without ϕ	71.6	68.5	68.5	68.3	72.4	69.9	2.82
	LFT with ϕ	76.2	73.3	74.9	74.2	74.2	74.6	1.52
	Gabor	68.8	65.7	62.8	64.4	69.4	66.2	4.27

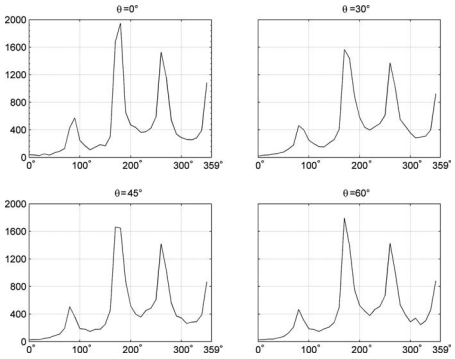

Fig. 2 Histograms of ϕ_2 for image D87 at four different orientations, θ=0, 30°, 45, and 60 deg.

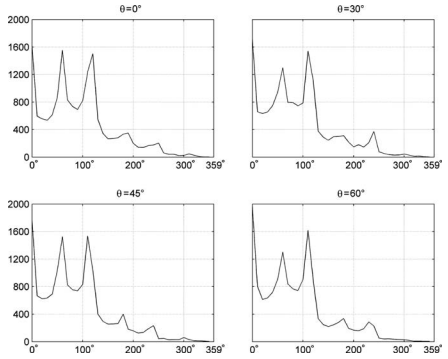

Fig. 3 Histograms of ϕ_3 for image D87 at four different orientations, θ=0, 30°, 45, and 60 deg.

$$\Delta\theta_k = -\frac{\pi}{4}km \tag{7}$$

in the Fourier domain: hence, where $\Delta\theta_k$ represents the shift in $\angle X_k$. The phase shift in $\angle X_1$ is given by

$$\Delta\theta_1 = -\frac{\pi}{4}m = \psi. \tag{8}$$

Intuitively, the change in the local image-gradient angle δ is equal to the angle of rotation at point P_{00} (ψ) that causes equal change in $\angle X_1$. Comparing Eqs. (7) and (8) gives the phase shift in $\angle X_k$ as

$$\Delta\theta_k = k \times \Delta\theta_1. \tag{9}$$

Therefore, the phases $\angle X_2$ and $\angle X_3$ are adjusted accordingly against the rotation by subtracting the local image-gradient angle δ as in Eq. (10). For $k \in \{2,3\}$,

$$\phi_k = \angle X_k - k\angle X_1, \tag{10}$$

where ϕ_k represents the rotation-compensated phase $\angle X_k$, and $\angle X_1$ replaces δ.

3 Experimental Results

3.1 *Rotation Invariance of the Phase Features*

All the images from the BA were rotated to 30, 45, 60, and 90 deg, and histograms of ϕ_2 and ϕ_3 were computed at each orientation. Table 1 shows the XCC as a similarity measurement between the histograms corresponding to 0 deg and to 30, 45, 60, and 90 deg averaged over all the images from the BA. As an example, Figs. 2 and 3 show the histograms of ϕ_2 and ϕ_3, respectively, for the image D87 from BA. All the histograms appear the same and do not exhibit any left or right shift, indicating that the two phases are highly rotation invariant. We also experimented with the features extracted from the circular neighborhood suggested in Ref. 2 and found that they perform worse than those extracted from the square neighborhood.

3.2 *Texture Recognition*

Each of the 107 texture images from the BA was oriented at 0, 30, 45, 60, and 90 deg. Then, 16 subimages measuring 128×128 pixels were cropped from each one of the 107 $\times 5$ images, giving a total of 8560 images.[4] Recognition was performed on this set using the LFH-based feature set without phase features, with phase features, and with texture features based on 30 Gabor filters.[4,5] Reference 6 is a more recent work that proposes exactly the same filters but with a new distance metric that cannot be used for rotation-invariant recognition or retrieval. Table 2 presents the overall and orientation-wise texture recognition results, showing that the LFH-based features with phases perform the best in terms of accuracy and the rotation variance (RV).[4]

4 Effect of Noise

Reference 4 found that the LFT-based texture features exhibit les noise immunity than the features based on Gabor filters. However, our latest results show that the LFT-based features perform even better when extracted from images quantized to only 32 gray levels. Considering this, we expect the proposed features to be more noise resistant than these were without image-quantization as in Ref. 4.

5 Conclusion

The earlier feature set based on LFH does not use phases of the DFT coefficients as texture features because the phases are sensitive to image orientation. To introduce rotation invariance in the features, we showed that the process of extracting phase features can be guided by the local image gradient. This was achieved by simply subtracting the local image-gradient angle obtained from the 1-D DFT itself, so that the features become self-compensating. This computationally simple and cost-effective method proved useful in making the LFH-based texture features robust against image rotation. The new feature set including the phase features exhibits more rotation invariance and yields higher recognition rates than the one without phase features.

References

1. M. Varma and A. Zisserman, "Texture classification: are filter banks necessary?," *Proc. Conf. Comp. Vis. Pattern Recog.*, 2, 691–698 (2003).
2. H. Arof and F. Deravi, "Circular neighborhood and 1-D DFT features for texture classification and segmentation," *IEE Proc. Vision Image Signal Process.* **145**, pp. 167–172 (1998).
3. F. Zhou, J.-F. Feng, and Q.-Y. Shi, "Texture feature based on local fourier transform," *Proc. EEE Conf. Image Process*, vol. 2, pp. 610–613 (2001).
4. A. A. Ursani, K. Kpalma, and J. Ronsin, "Texture features based on Fourier transform and Gabor filters: an empirical comparison," *Int. Conf. Mach. Vis.*, vol. 145, pp. 67–72 (2007).
5. B. S. Manjunath and W. Y. Ma, "Texture features for browsing and retrieval of image data," *IEEE Trans. Pattern Anal. Mach. Intell.*, **18**(8), 837–842 (1996).
6. P. Wu, B. S. Manjunath, S. Newsam, and H. D. Shin, "A texture descriptor for browsing and similarity retrieval," *Signal Process. Image Commun.*, **16**, 33–43 (2000).